

# Changing the Anchor Density of a Swollen Polymer Brush at the Interface of Two Immiscible Liquids

R. Teppner and H. Motschmann\*

Max-Planck Institute of Colloids and Interfaces, Rudower Chaussee 5, D-12489 Berlin, FRG

Received December 11, 1997

**ABSTRACT:** Diblockcopolymers of polystyrene and poly(oxyethylene) were adsorbed at the toluene/water interface. The short water soluble poly(ethylene oxide) block anchors the polymer at the interface, whereas the long nonadsorbing Polystyrene block remains in toluene in good solvent conditions. The adsorption layer adopts a brushlike conformation, and the system serves as a model for end-adsorbed polymers. A film balance especially designed for liquid–liquid interfaces allows a compression of the adsorption layer via a movable barrier and allows the control of the anchor density of the polymer. The balance was optimized for optical reflection measurements and enables the simultaneous determination of the surface tension. Ellipsometric measurements reveal that the density of the adsorption layer does not change with compression. However, the thickness of the layer depends linearly on the anchor density. This finding is in reasonable agreement with the prediction of the scaling laws.

## I. Introduction

A polymer brush is composed of flexible polymers anchored at one end to an interface.<sup>1</sup> The average spacing of the anchor groups is significantly less than the characteristic dimensions of the undisturbed dissolved polymer in solution. These peculiarities lead to the stretched brushlike conformation of the polymer.

Many diblock copolymers form brushlike adsorption layers.<sup>2</sup> For this to occur, a necessary requirement is a different affinity of both blocks for the interface.<sup>3</sup> The short block, or the end group, possesses a high affinity for the interface and anchors the polymer whereas the long block is nonadsorbing and remains in good solvent conditions. The adsorption layer is homogeneous and the segment concentration within the adsorption layer matches that of polymer solutions within the semidilute regime.

Many practical applications in the field of colloids and ceramics depend on a deliberate control of interfacial properties.<sup>4,5</sup> Polymer brushes are used as efficient stabilizers of colloidal particles.<sup>6</sup> The brushlike adsorption layer prevents an aggregation and subsequent precipitation of individual particles. With the overlap of the adsorption layer of different particles, a strong repulsive force occurs. The nature of this force is purely osmotic and is caused by an increase of the number density of polymer segments.<sup>7</sup> A crude estimation reveals that only a few percent of the total volume within the adsorption layer is occupied by the polymer and the main part consists of solvent that governs many physical properties of the adsorption layer.

Owing to their importance, considerable effort has been spent in the theoretical description of dynamic and static properties of polymer brushes.<sup>2,8</sup> The first sound treatment was provided by Alexander and deGennes and was based on scaling arguments.<sup>9</sup> A dimensional analysis yields power laws relating particular quantities of the adsorption layer, e.g., its thickness  $t$ , and the anchor density  $\sigma$  with molecular properties (e.g., degree of polymerization  $N$ ). The treatment introduces the concept of blobs, which assumes two distinct length scales in a polymer. Below the blob diameter, the

excluded volume is important whereas on length scales beyond the blob diameter all correlations are lost. The adsorption layer is then treated as a melt of blobs. This concept was, despite certain simplifying assumptions, quite successful in the description and prediction of polymer properties. The main findings of the scaling theory were also verified by Milner with more sophisticated approaches based on an analytical local self-consistent mean field theory.<sup>10</sup> This analysis provided additional insight into the adopted segment concentration profiles. The predicted segment concentration profile resembles a parabola, rather than the step function obtained by Alexander and deGennes. Monte Carlo investigations were used to study dynamic properties of polymer brush formation and in this context also questions concerning the reversibility and exchange of individual polymers were addressed.<sup>11</sup>

The clarity of the predictions have appealed to many experimentalists and numerous studies deal with the verification of scaling laws.<sup>12–15</sup> In those studies suitable polymers were adsorbed onto solid supports and the mass coverage and the thickness were determined. Due to the peculiarities of the system, mainly optical techniques were employed and the molecular weight of the samples had to be varied. The main drawback of these measurements is that the anchor density of the polymer cannot be controlled. The adsorption process stops at a given surface coverage. Each polymer penetrating the layer has to overcome an osmotic pressure that limits the equilibrium surface coverage.<sup>2</sup>

In the present contribution, instead of solid supports we used the interface of two immiscible liquids as an adsorption site for diblock copolymers with asymmetric block length. This arrangement offers decisive advantages as compared to solid supports. Liquid–liquid (lq/lq) interfaces are well-defined and of fairly simple symmetry with a known chemical composition. These conditions do not necessarily hold for solid supports. The surface composition of a solid support deviates from its bulk chemistry and also depends strongly on the applied cleaning procedure. Furthermore the interpretation of the findings can be complicated by roughness, grain boundaries, and anisotropies of the sample. However,

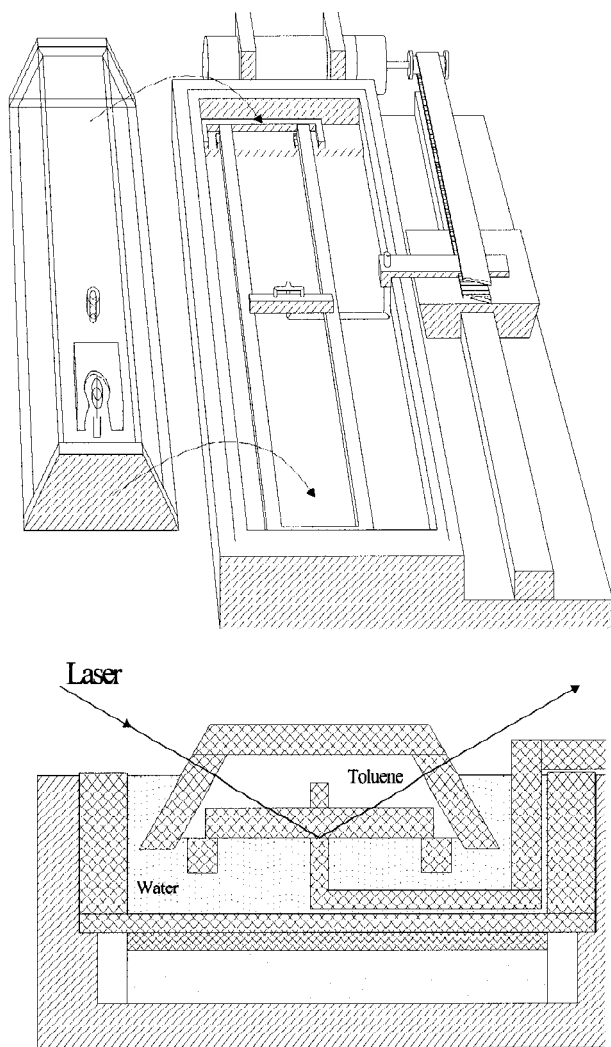


**Figure 1.** (a) Schematic diagram of the layout of the system consisting of the specially designed trough and the insertable quartz cell. The quartz cell that contains the organic phase is held in place by Teflon mounts. Also shown in the diagram is the Wilhelmy system and the inlet tube for the oil phase. The troughs barrier is connected by a quartz-U-bar to a translation stage equipped with a dc motor. This arrangement eliminates disturbance of the interface during compression and expansion cycles and prevents any corrosive parts from being exposed to both phases of interest. (b) Cross sectional area of the film balance for liquid-liquid interfaces: The aqueous medium is placed in the main quartz container, and the trapezoidal cell provides the housing for the volatile hydrocarbon. As a result of this arrangement, water is partially displaced by the less dense hydrocarbon and an airtight housing for the hydrocarbon is produced. The angle of  $59^\circ$  of the cell was chosen for ellipsometric purposes.

the most striking advantage of the lq/lq interfaces is the possibility of manipulating and controlling the anchor density of the adsorbed species. For this reason a Langmuir type film balance for liquid-liquid interfaces was designed. The balance was optimized in order to apply optical reflection techniques under well-defined experimental conditions. The adsorption layer formed under equilibrium conditions was compressed and the mass coverage and the thickness were monitored by ellipsometry. These findings are compared with the predicted scaling law.

## II. Experimental Background

**A. Film Balance.** Figure 1 shows a sketch and a cross sectional area of the film balance. The trough, barrier, and

rim are made of fused silica as well as the trapezoidal cell, which contains the organic phase. Fused silica is the material of choice, because (a) it does not cause any contamination of the solution as, e.g., by a release of ions, (b) it can be efficiently cleaned using aggressive acidic and oxidizing solutions, and (c) it can be easily hydrophobized or hydrophilized by well-established silanization procedures. The latter can be exploited to prevent leakage of the monolayer at the liquid-liquid interface. Best results were obtained if all sides of the barrier and rim are hydrophobic, with the exception of the lower surface of the barrier and the side faces of the rim. The film balance consists of a movable barrier and rims. The barrier is connected via quartz-U-bar with a translation stage equipped with a dc motor and optical encoder. The cell, which provides the housing for the volatile hydrocarbon, and the rims are fixed in a Teflon holder, as shown in Figure 1. For the experiments, water is first filled in the main container and, subsequently, the hydrocarbon is injected in the trapezoidal cell. The water is partially displaced by the less dense hydrocarbon and as a result of this arrangement an airtight housing for the volatile organic phase is produced. Details about the trough and a demonstration of its functionality can be found in ref 16.

**B. Optical Characterization.** All relevant design features of the optical setup (Multiskop, Optrel, Germany) are discussed in detail in ref 17. We used only the ellipsometry module in a Null ellipsometer mode using a laser, polarizer, compensator, sample, analyzer arrangement. A 2 mW HeNe laser was used as a laser light source. Precise ellipsometric measurements require that the incident light strikes the entrance cell window under normal incidence to prevent changes in the state of polarization by transition or adsorption layers.<sup>18</sup> The angle of the entrance windows of our cell is  $59^\circ$ , chosen such as to provide a sufficiently high sensitivity. During the manufacture state of the cell windows, care was taken to avoid birefringence. The remaining birefringence was analytically corrected in the data analysis.

**C. Data Analysis. Inversion of the Ellipsometric Equation.** Two quantities  $\Delta$  and  $\Psi$  are measured in an ellipsometric experiment. Both are related via the basic equation of ellipsometry with the optical properties of adsorption layer.

$$\tan \Psi e^{i\Delta} = \frac{R_p}{R_s} = f(n, t) \quad (1)$$

$R_p$  and  $R_s$  are the reflectivity coefficient parallel and perpendicular to the plane of incidence and calculated on the basis of a Fresnel theory.<sup>18</sup> The reflectivity coefficients are a function of the unknown refractive indices and layer thickness of the adsorption layer. All optical properties of the ambient media can be determined beforehand and only the two film parameters remain as unknowns.

Unfortunately, there is no direct and unique way to invert eq 1 to determine the unknown layer parameters, and especially, the quite frequently used algorithm proposed by McCrackin lacks numerical stability.<sup>19</sup> We interpreted our data using the exact Fresnel equations for stratified media. The experimental ellipsometric angles  $\Delta$  and  $\Psi$  are a function of the two unknown film parameters  $n$  and  $t$ . There are several  $n, t$  combinations that yield the same observable quantity and the experimental data should be represented as contour lines  $t(n)$ . The intersection point of the contour lines for  $\Delta$  and  $\Psi$  provides the unknown film parameter.<sup>20</sup> Furthermore, the experimental accuracy in the determination of the ellipsometric angles was taken into account by a calculation of the intersection points corresponding to  $\Psi^-, \Delta^-, \Psi^+, \Delta^-, \Psi^-, \Delta^+$ , and  $\Psi^+, \Delta^+$ . The + or - superscripts stand for  $\pm$  experimental error, which was about  $0.02^\circ$ . This procedure gives also direct insight into the ambiguity of the data interpretation. The error in  $n$  and  $t$  increases at low surface coverage.

**Determination of the Adsorbed Amount  $\Gamma$ .** The refractive index of a polymer solution increases linearly with its concentration:

$$n = n_0 + \frac{dn}{dc}c \quad (2)$$

The refractive index of the polymer solution is  $n$ , the refractive index of pure toluene is  $n_0$  and  $c$  is the concentration of the solution. The refractive index of polymer solutions of different concentration was determined with an Abbe refractometer and the increment  $dn/dc$  was determined to be  $dn/dc = 1.02 \times 10^{-4}$  mL/mg.

As pointed out, an adsorption layer and polymer solutions in the semidilute regime possess some similarities. The adsorbed amount  $\Gamma$  can be calculated using the above determined  $dn/dc$ :

$$\Gamma \frac{(n - n_0)}{dn/dc} t = c_0 t \quad (3)$$

where  $t$  stands for the thickness of the layer and  $c_0$  refers to the average concentration within the adsorption layer. In unfavorable cases there is an inherent ambiguity in the determination of  $n$  and  $t$  that cancels out in the determination of  $\Gamma$ .  $\Gamma$  reflects the zero moment of the distribution function characterizing the adsorption layer. This quantity can always be calculated from ellipsometric measurements; however, conclusions about higher moments, as for instance the layer thickness, concentration profiles, and so on, should be very critically and carefully analyzed to avoid an overinterpretation of the data. A sound treatment of this problem can be found in the book of Lekner.<sup>21,22</sup>

**D. Materials.** A diblock copolymer of polystyrene (PS) and poly(oxyethylene) (PEO) was used. It was purchased from Polymer Laboratories U.K. The number of monomers of the long PS block is 1700, the number of monomers of the poly(ethylene oxide) block is 64. The polymer is monodisperse with a ratio of  $M_w/M_n = 1.09$ . Polystyrene is in good solvent condition in toluene and does not dissolve at all in water, whereas PEO can be dissolved in water. The radius of gyration is about 120 Å, as determined by static light scattering. Toluene (p.A.) was purchased from Sigma Aldrich and used as received. The water was specially purified water (Milli-Q) with a resistivity of 18 MΩ cm.

**E. Experimental Procedure.** Before assembling the system, each individual part of the film balance was thoroughly cleaned. The applied procedure consists of several steps: (1) aqueous tenside solution in an ultrasonic bath for 1 h, (2) rinsing with Milli-Q water, (3) 2-propanol in an ultrasonic bath for 1 h, (4) rinsing with Milli-Q water.

The film balance was assembled and filled with both liquids. The constancy of the ellipsometric signal and the surface pressure with time was monitored. Any trace impurities with an amphiphilic character would be detected as well as temperature drifts within the system. The temperature was controlled via a thermostat. Once a well-defined pure toluene/water interface was established and characterized, a solution of the dissolved block copolymer in toluene was injected in the organic phase. Care was taken to ensure that all solutions are at the very same temperature (20 °C) to minimize convection. The concentration of the polymer in the toluene phase is about 0.0067 mg/mL. The organic and the aqueous phase remain clear. Therefore, micelles are not formed or their concentration is so low that they do not have an impact on ellipsometric measurements. Once the equilibrium surface coverage of the adsorbed polymer at the lq-lq interface is established, the actual experiment consisting of several compression and decompression cycles was started.

### III. Results and Discussion

The adsorption process of a block copolymer at the toluene/water interface is a two-stage process and possesses features similar to those of adsorption on solid supports.<sup>12</sup> The main fraction of the polymer is adsorbed in a diffusion-controlled process, and the equilibrium surface coverage is achieved within a couple of

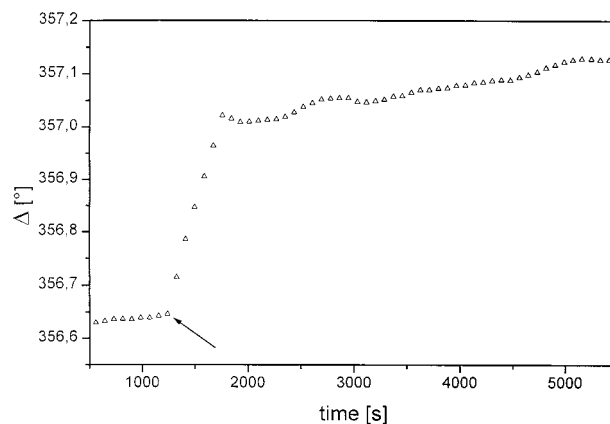


**Figure 2.** Adsorption of PS-PEO diblock copolymers at the toluene-water interface. The plot shows the time evolution of the ellipsometric angle  $\Delta$ , which is in our arrangement proportional to the adsorbed amount at the interface. The arrow indicates the point of injection of dissolved block copolymer PS-PEO. The main fraction is transferred in a diffusion-controlled process to the interface. Equilibrium is achieved within a few hours.

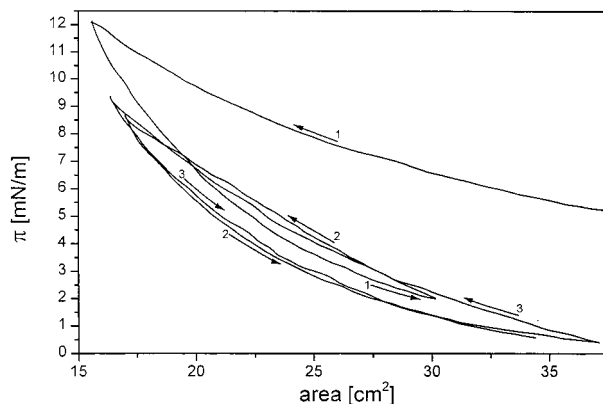


**Figure 3.**  $\pi, A$  isotherm of PS-PEO at the toluene water interface. The recorded isotherm of the first compression deviates from all subsequent compression/expansion cycles. After the first compression, only slight hysteresis is observed between all further compression and expansion runs and therefore this state was used in the further analysis.

hours. The adsorption stops at a given coverage that depends on the molecular weight of the nonadsorbing block. The limiting process is the osmotic repulsion, which hinders further polymers from penetrating the adsorption layer. Figure 2 shows the change with time in the ellipsometric angle  $\Delta$  due to the adsorption. The arrow indicates the injection of the polymer solution. In our arrangement, the measured quantity  $\Delta$  is directly proportional to the adsorbed amount at the interface.

After having established an equilibrium state, compression of the monolayer began. The corresponding isotherms are shown in Figure 3. The isotherm recorded for the first compression differs from all subsequent compression/expansion cycles. The first compression leads to an onset in the surface pressure at higher areas per molecules compared to subsequent runs. After the first compression the isotherms are reversible with little hysteresis between compression and expansion cycles. Hence in this regime a significant loss of material with compression can be ruled out and, furthermore, the adsorption layer is in a well-defined state. A possible and unwanted scenario would be a continuous loss of material with compression due to the formation of inverse micelles, which leave the interfacial

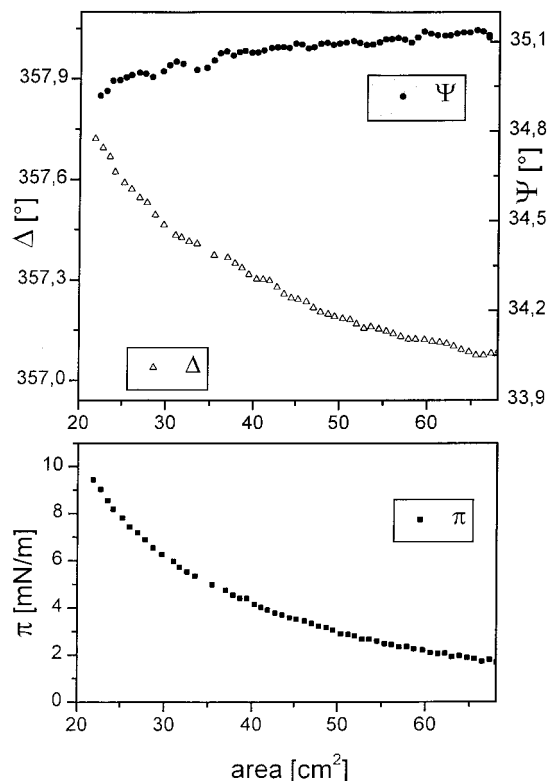


**Figure 4.** (Upper figure) dependence of the ellipsometric angles  $\Delta$  and  $\Psi$  with compression of the adsorption layer. There are only minor but clearly resolvable changes in  $\Psi$ . (Lower figure) corresponding plot for the surface pressure  $\pi$ .

area and diffuse in the toluene phase. Obviously, this does not happen in our experiment. The reason for the difference between the initial compression and subsequent compression cycles is not yet understood. One is tempted to explain this in terms of the adsorption or formation of micelles in the interfacial area or by the formation of interdigitating polymer chains with compression. Since a good reversibility and reproducibility of all data is given after the first compression, we used this state for further analysis of polymer brush features.

The surface pressure  $\pi$  and the ellipsometric angles  $\Delta$ ,  $\Psi$  are continuously recorded with compression. Figure 4 presents a representative plot. The area refers to the state before compression and is not normalized by the adsorbed amount as determined by ellipsometry measurements. With compression a change in both ellipsometric angles  $\Delta$  and  $\Psi$  can be observed. The angle  $\Psi$  measures the ratio of the reflectivity for  $\hat{p}$  and  $\hat{s}$  polarization (see eq 1). The presence of a thin layer with a refractive index close to the organic phase has only a minor impact on the observed reflectivity. Nevertheless there are slight changes in  $\Psi$  which can be clearly resolved. These data can be used to determine both  $n$  and  $t$  of the adsorption layer. However, at lower surface coverage some ambiguity in the data interpretation remains as previously discussed.

The ellipsometric data were analyzed on the basis of the described algorithm and the refractive index  $n$  and the thickness of the adsorption layer  $t$  were determined together with the error in both quantities. The area accessible to the polymer allows a calculation of the average spacing of the anchor groups. The relevant plot is shown in Figure 5. The refractive index  $n$  remains fairly unchanged with compression of the adsorption layer. This implies that the average density of the

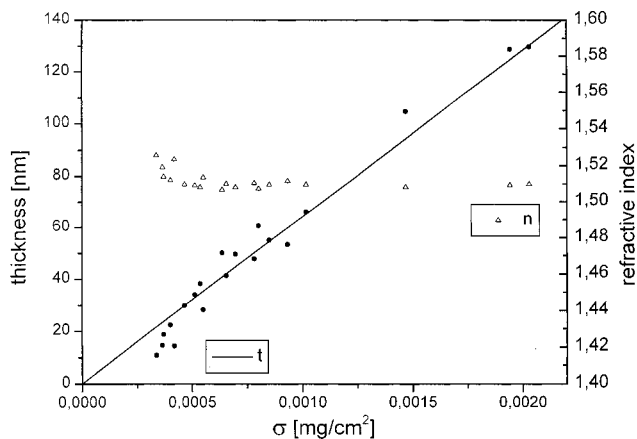


**Figure 5.** The ellipsometric angles  $\Delta$  and  $\Psi$  were used for the determination of refractive index  $n$  and thickness  $t$  of the adsorption layer. The calculation is based on Fresnel theory for stratified media and uses no approximations. Furthermore, the experimental error was taken into account to estimate the remaining ambiguity of the calculated  $n$  and  $t$ . Both quantities are plotted as a function of the anchor density  $\sigma$  of the polymer, which was determined by the area accessible to the polymer. The straight line represents a fit to the data according to the prediction of the scaling law of Alexander and deGennes.

polymer brush is independent of the average spacing of the anchor group. As a result, significant changes in layer thickness occur. With compression, the thickness increases by a factor of 6. The dependence between thickness and anchor density  $\sigma$  can be reasonably approximated by a straight line. The straight line in Figure 5 is a best fit to the experimental data based on the prediction of the scaling law of Alexander and deGennes derived for polymer melts. This relation also describes reasonably well our experimental findings for the brushlike adsorption layer in good solvent conditions. It states that the thickness  $t$  should be directly proportional to the anchor density  $\sigma$  of the polymer within the adsorption layer and to the degree of polymerization  $N$ . There are some systematic deviations at lower surface density but in general a reasonable agreement between experimental quantities and theory can be found. The adsorbed amount allows a calculation of the area per molecule,  $A$ , within the adsorption layer. This can be compared to the geometrical dimensions of the undisturbed polymer in solution, as determined by the light scattering experiment. The radius of gyration of the polymer in toluene is 12 nm and hence a random coil should occupy an area  $A_0$  of 450 nm<sup>2</sup>. The ratio of  $A/A_0$  varies from 0.4 before compression to 0.05 in the highly compressed state. The adsorption layer is in a brushlike regime and compression of the monolayer gives access to a broad range of anchor densities  $\sigma$ . The mean field theory of Milner predicts that, with compression, solvent is squeezed out of the adsorption layer. Our data do not provide evidence for this since the refractive index remains constant with compression.

#### IV. Summary and Conclusion

The interface between two immiscible liquids is an ideal tool for the investigation of adsorption processes of polymers and to study equilibrium properties of the adsorption layer. Fluid–fluid interfaces are of fairly simple symmetry with a well-defined chemical composition as compared to the interface between a solid and a liquid. The decisive advantage is the possibility of deliberately controlling the anchor density of the ad-

sorbed polymers by means of a movable barrier. The design of the film balance is optimized for optical reflection techniques. Ellipsometric measurements reveal that the thickness of a polymer brush depends linearly on the anchor density of the polymer whereas the segment density remains unchanged. The arrangement can be used to investigate further classes of polymer, e.g., polyelectrolyte brushes, and to address the influence of the quality of the solvent on the brush.<sup>23,24</sup> The same arrangement can also be employed to use evanescent wave ellipsometry for a retrieval of the segment concentration profile within the adsorption layer.

**Acknowledgment.** The authors thank Prof. Möhwald for stimulating discussions, also Prof. Eichler (TU Berlin) for the supervision of the diploma thesis of Randolph Teppner.

### References and Notes

- (1) Milner, S. T. *Science* **1991**, *251*, 905. De Gennes, P. G. *Macromolecules* **1980**, *13*, 1069.
- (2) Halperin, A.; Tirrell, M.; Lodge, T. P. *Adv. Polym. Sci.* **1992**, *100*, 31.
- (3) Siquera, D. F.; Reiter, J.; Breiner, U.; Stadler, R.; Stamm, M. *Langmuir* **1996**, *12*, 973.
- (4) Sanchez, I. C., Ed. *Physics of Polymers and Interfaces*; Butterworth-Heinemann: Boston, 1992.
- (5) Fleer, G. J.; Cohen Stuart, M. A.; Scheutjens, J. M.; Cosgrove, T.; Vincent, B. *Polymers at Interfaces*; Chapman and Hall: London, 1993.
- (6) Napper, D. H.; *Stabilization of Colloidal Dispersions*; Academic Press: London 1983.
- (7) Taunton, H.; Toprakcioglu, C.; Fetters, L. *Nature* **1988**, *332*, 712. Toprakcioglu, C.; Ansarifar, M.; Stamm, M.; Motschmann, H. *Colloids Polym. Sci.* **1991**, *83*, 1993.
- (8) Szleifer, I.; Carignano, M. A. *Adv. Chem. Phys.* **1996**, *94*, 165.
- (9) Alexander, S. J. *J. Phys. Paris* **1977**, *38*, 983. De Gennes, P. G. *J. Phys. Paris* **1976**, *37*, 1443. deGennes, P.-G. *Macromolecules* **1980**, *13*, 1069.
- (10) Milner, S. T.; Witten, T. A.; Cates, M. E. *Europhys. Lett.* **1988**, *5*, 413. Milner, S. T.; Witten, T. A.; Cates, M. E. *Macromolecules* **1988**, *20*, 2610.
- (11) Kopf, A.; Baschnagel, J.; Wittmer, J.; Binder, K. *Macromolecules*, in press.
- (12) Motschmann, H.; Stamm, M.; Toprakcioglu, C. *Macromolecules* **1991**, *24*, 3681.
- (13) Wang, W. P.; Barton, S. W. *J. Phys. Chem.* **1995**, *99*, 2845.
- (14) Goedel, W. A.; Heger, R. *Prog. Colloid Polym. Sci.* **1997**, *105*, 160. Heger, R.; Goedel, W. A. *Macromolecules* **1996**, *29*, 8912.
- (15) Halperin, A.; Joanny, J. F. *J. Phys. II* **1991**, *1*, 623.
- (16) Teppner, R.; Harke, M.; Motschmann, H. *Rev. Sci. Instrum.* **1997**, *68* (11), in press.
- (17) Harke, M.; Teppner, R.; Schulz, O.; Orendi, H.; Motschmann, H. *Rev. Sci. Instrum.* **1997**, *68* (8), 3130.
- (18) Azzam, R. M.; Bashara, N. M. *Ellipsometry and Polarized Light*; North-Holland Publication: Amsterdam, 1979.
- (19) McCrackin, F. L.; Colson, J. P. *Natl. Bur. Stand. Misc. Oubl.* **1964**, *256*, 363.
- (20) Reiter, R.; Motschmann, H.; Orendi, H.; Nemetz, A.; Knoll, W. *Langmuir* **1992**, *8*, 1784.
- (21) Lekner, J. *Theory of reflection*; Martinus Nijhoff Publishers: Boston, Lancaster, 1987.
- (22) Harke, M.; Stelzle, M.; Motschmann, H. *Thin Solid Films* **284**, *412*, 1996.
- (23) Zhulina, E. B.; Borisov, O. V.; Pryamitsyn, V. A. *J. Colloid Interface Sci.* **1990**, *137*, 495.
- (24) Martin, J. I.; Wang, Z. G. *J. Phys. Chem.* **1995**, *99*, 2833.

MA9718053